JOURNAL OF MATERIALS SCIENCE 31 (1996) 2109–2116

Adhesion of nylon-6 on surface treated aluminium substrates

KAI-TAK WAN*, A. DI PRIMA, LIN YE, YIU-WING MAI
Centre for Advanced Materials Technology, Department of Mechanical and Mechatronic Engineering, University of Sydney, NSW 2006, Australia

The adhesion between nylon-6/aluminium is discussed in terms of mechanical interlocking mechanism on a microscopic scale. A new "shaft-loaded" blister test was adopted to measure simultaneously the adhesive properties of thin nylon-6 films. Fracture toughness is also measured by a double cantilever beam geometry. Variables including polymer film thickness, hot-press conditions and durability are also investigated.

1. Introduction

Technological advances in microelectronics require good adhesive properties of thin polymeric and ceramic thin films on many critical surfaces. For instance, metallic contacts, dielectric in capacitors, packaging against mechanical damage, optical and magnetic thin films, etc. all require good adhesion performance to be engineering reliable. Debonding of such films caused by contaminants, intrusion of environmental species at fractured interfaces, or residual thermal stress in the fabrication process, leads to breakdown of electronic components which could be costly to repair. It is therefore necessary to probe into the adhesion mechanism and to quantify the adhesive strength.

The mechanism of adhesion between polymer thin film and a rigid metal/ceramics substrate can be divided into two different trends, one along the line of interfacial chemistry [1, 2] and the other mechanical interlocking [3, 4].

Adhesion between polymer, ceramics and metal is strenuous due to the different bonding mechanisms of the atoms or molecules involved. Macropolymer molecules are bonded together via weak van der Waals forces and/or hydrogen bonding; the atomic structure of ceramics is, on the other hand, governed by strong covalent bonds; metallic ions are pulled together by the overlap of electron clouds. When these vastly different materials combine to form a composite, the adhesion at the dissimilar interfaces might be the consequence of a combination of the above forces, or probably none of them. For instance, in some polymer composite blends, the formation of a crystallized interlayer increases the mechanical communication between the matrix and the fibres and thus give better adhesion [5]. Thus studies of the dissimilar interfaces hold an important key to improving the reliability of engineering materials. Enhancement of adhesion can be achieved by the addition of coupling agents, ion beam stitching, pre-deposition sputtering and surface treatment [3, 6] of the substrate, etc.

The physical aspects are equally important in adhesion performance. It is now believed that a dissimilar interface must be considered as a three-dimensional entity, rather than a smooth two-dimensional plane [3]. A roughened metal or ceramic surface has a significant positive effect on the "mechanical interlocking" of a polymer overlayer. The interlayer, or sometimes known as "interphase", consists of metal oxide protrusions from the metal surface and polymer fingers locked into the valleys. When a polymer is deposited on such a surface, the penetrating fingers of either side provide a much larger adhesive surface as well as "anchors". In this paper, we will concentrate on the topological control of the substrate surface and its effect on the overall adhesion at metal/polymer interfaces.

The literature on interfacial physics and chemistry is voluminous, yet standard ways to quantify adhesion are controversial and non-conclusive. The conventional peeling test leads to serious plastic deformation because of high angle bending at the crack front [7]; pin pull tests are difficult to quantify in terms of fracture mechanics [6]; micro-indentation is restricted to very weak adhesion and interpretation of experimental data is difficult [8]; other novel methods do not conform to conventional fracture mechanics and are much restricted by interpretation. The now celebrated "blister test" is by far the best and only method which yields consistent adhesion measurements based on fracture mechanics [9, 10].

A blister specimen is fabricated by first depositing the polymeric film on the specified substrate. A hole is drilled or chemically etched through the substrate reaching the interface. A fluid of either gas or liquid is then allowed to pressurize the overlying film until a blister crack is formed. The relation between the applied pressure and the debonding area thus gives

* Now at the Department of Mechanical Engineering, Hong Kong University of Science and Technology, Clear Water Bay, Hong Kong.

0022–2461

a measure of the adhesive strength. However, the now available fracture mechanics model is strictly restricted to elastic deformation only, though plastic yielding is almost unavoidable in a strong interface. An alternative mode of blister test is one driven by a mechanical shaft [11], in that, both elastic and plastic moduli, plastic yield strength, and energy of adhesion can all be simultaneously measured in a single experiment. We will adopt the shaft-loaded blister test in the present work. Further control experiments using the double cantilever beam (DCB) geometry was also carried out.

We also investigated the several controlling factors which influence the interfacial interlocking using DCB geometry, such as the hot-pressing temperature of the specimens, and exposure of the interface to environments.

2. Experiment

Polyamides and polyimides on metal surfaces and silicon wafers are of special interest in the microelectronics industries due to their wide application. We will examine the dissimilar interfaces of nylon-6/aluminium as an example.

2.1. Materials

2.1.1. Nylon-6

The detailed chemical composition, preparation process, mechanical properties of bulk nylon-6 are well documented [12, 13]. Here we are only interested in the physical aspects of adhesion, so raw nylon-6 is used without any chemical treatment. It is well known that the polymer is hygroscopic and its water content has significant influence on the mechanical properties. When it is heated to its melting point at 223 °C, effervescence of water vapour occurs followed by oxidation which turns the polymer from clear to a brownish opaque colour. The nylon-6 used in our experiments was left in a vacuum oven at 70 °C overnight to get rid of the water and was then stored in a desiccator with copper sulphate anhydride. When it melted at elevated temperature, no effervescence was observed and the polymer remained clear. The melted nylon-6 solidified when the temperature dropped below 180 °C.

Nylon-6 was cut into rectangular sheets of approximately 10 cm × 0.5 cm and 2 mm thick. The stress–strain response was tested by a universal testing machine. The test was run several times with the crosshead speed in the range from 0.1 to 50 mm s^{-1}. The result is plotted in Fig. 1. The stress–strain responses of nylon-6 at various crosshead speeds almost coincided with one another. The elastic modulus was found to be 530 ± 30 MPa. When the yielding stress at 30 ± 3 MPa was reached, necking occurred at some unspecified position on the specimen, followed by drawing. The external load remained constant upon specimen elongation until the entire tensile bar was reduced to a uniform width, then the specimen broke. The post-yielding elastic modulus of a necked specimen was difficult to measure. However, it would be reasonable to assume that nylon-6 is perfectly plastic in the present work.

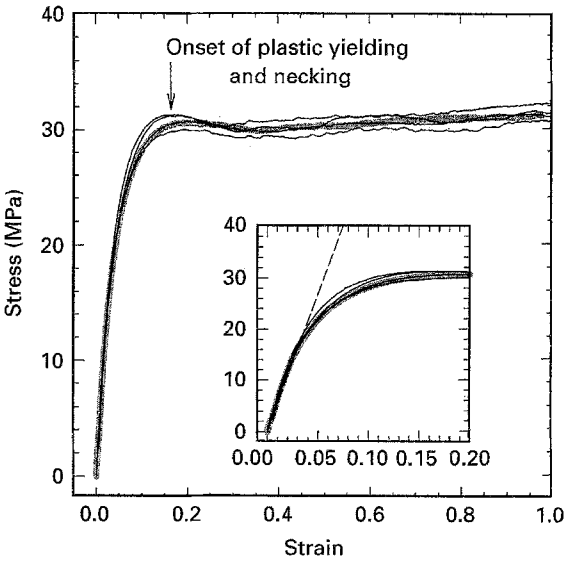

Figure 1 The stress–strain response of nylon-6 for crosshead velocity of 0.1, 0.5, 1.0, and 10.0 m s^{-1}. The grey line represents the average stress–strain behaviour. Plastic yielding and subsequent necking occurs once the strain reaches approximately 0.16. The inset shows an enlarged plot for strain from 0.0 to 0.2. The dotted line shows the linear elastic portion of the mechanical behaviour.

2.1.2. Aluminium surfaces

Fresh aluminium is oxidized spontaneously in air which leaves a thin oxide layer on the surface [14]. It is now believed that when a long-chain carbon polymer adheres to aluminium, the hydrogen on some radical groups of the polymer attach to the oxide film resulting in the formation of a hydroxyl group. It is such hydrogen bonding which gives rise to the adhesion. The metal oxide surface layer is thus essential to adhesion. Here we are only interested in the mechanical interlocking mechanism. The surface treatments described below are to modify the topology of the surface oxide layer to enhance adhesion.

Aluminium plates were polished to 1 μm finish. The plain surface was investigated along with three surface treatments [15]: (a) phosphoric acid anodization process, (b) sulphuric acid anodization process and (c) P2 etching process (sulpho-ferric etch). In treatment (a), the electrolyte was prepared by dissolving 160 ml of 85% phosphoric acid in 1 litre of deionized water. The aluminium plate was attached to the anode of a d.c. supply, with a carbon rod as the cathode. The d.c. voltage was applied stepwise to 10 V in 2–5 min and subsequently maintained at 10 V for 25 min at room temperature. In treatment (b), the electrolyte was a 10% sulphuric acid heated to 70–80 °C. The voltage across the electrodes was kept at 20 V for 10 min. In treatment (c), the etching solution consisted of 200 ml of concentrated sulphuric acid, 150 g of ferric sulphate, and deionized water to make up to 1 litre of solution. The aluminium plates were left dipped in the solution for 5 min at 60–65 °C. In all three treatments, the specimens were rinsed thoroughly in water

for 5 min before the polymer deposition. The mirror surfaces tarnished after surface treatment, due to the pitting of aluminium and growth of the oxide layer. Experiments were also carried out for aluminium plates dipped in the P2 etch for 1, 2, 4, and 6 min. The surfaces were left in laboratory air to dry before thin film deposition.

2.2. Shaft-loaded blister test

2.2.1. Specimen preparation

A small lump of nylon-6 was left on a treated aluminium plate of dimensions 15 mm × 15 mm and 2 mm thickness. The specimen, covered with thin aluminium foil, was then put on a hot stage. The temperature was slowly raised at a rate of $1\,^{\circ}C\,s^{-1}$ until it reached 240 °C, and held constant for 3 min before cooling at $-1\,^{\circ}C\,s^{-1}$ to room temperature at 25 °C. The thickness of the nylon-6 film deposited on the aluminium substrate was made to be in the range of 100–200 μm and uniform over the entire surface. The film remained clear as it had prior to melting. Occasionally some films were oxidized and turned a brownish opaque colour. Such specimens were discarded.

2.2.2. Shaft-loaded blister test

An axisymmetric vent of diameter 11 mm was bored through the plate by a mechanical drill. In the drilling process, a small amount of plastic deformation was induced at the centre of the film.

A stainless steel cylindrical shaft with parallel flat ends and diameter of 1 mm was attached to the load cell of a universal testing mechine (Fig. 2a). A steel ball of 1 mm diameter was left in the vent leading to the blister. The shaft was aligned to touch the steel ball and had a crosshead speed of $0.1\ mm\ min^{-1}$. The applied load P versus shaft displacement w_0 was recorded simultaneously throughout the entire loading process. The load was removed at intervals allowing the measurement of the debonding radius a. The blister was then re-loaded. Such loading–unloading–reloading cycle was repeated several times for each blister with an ever increasing blister radius.

An alternative blister test is a modified indentation technique (Fig. 2a and b). Since the adhesive strength can be determined by the applied load P and the corresponding debonding radius a only, we do not have to measure the blister central deflection w_0 which can be deduced from P and a. In this method, after a fixed P is applied, $2a$ is measured at the load removal. No record of w_0 will be kept. In most microhardness testers, P is usually limited to between 10 g and 1 kg and the maximum distance travelled by the indenter is constrained. This presents another restriction of the indentation technique. In spite of all the limitations and constraints, the test method is simple to carry out.

A special indenter with a round ended shaft was made with a radius of 1 mm (Fig. 2a). The specimen with the thin film facing down was put on a ring support so that the path of the shaft would not be obstructed. When the indentation load was removed,

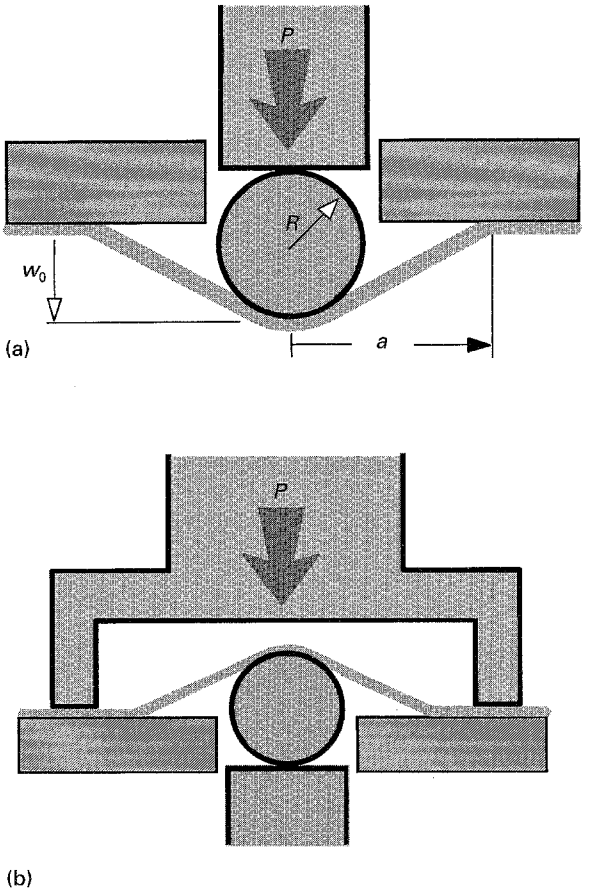

Figure 2 Sketch of a shaft loaded membrane blister. (a) An external P pushes against a steel ball of radius R which in turn drives a debonding blister of radius a. (b) A blister is supported by a stationary shaft with a spherical end. An external load P is applied via a cylindrical shell of radius much bigger than the blister radius.

the specimen was flipped over and the debonding radius measured under an optical microscope. A complementary alternative was to use a cylindrical shell indenter (Fig. 2b). While the blister was resting on a stationary protruding round ended shaft, the indentation load was applied via the axisymmetrically placed shell indenter. On removal of the external load, the debonding radius could be measured without displacing the specimen. Subsequent measurements were made by increasing P. Most of the adhesion energy measurements quoted later will be based on the indentation technique.

The adhesion at the nylon-6/aluminium interface was also measured in the presence of water. A drop of water was used to fill the blister volume before loading. The specimens were then stored for 10 months in laboratory air to assess the influence of ageing.

2.3. Double cantilever beam configuration

Aluminium bars of dimensions 150 mm × 25 mm and 10 mm thickness were polished to 30 μm finish (Fig. 3). Here only the plain, P2 etching process was investigated. Two sheets of aluminium foil were sandwiched between two nylon-6 sheets to provide a pre-crack from one end. The stack was then placed in between two metal bars before hot-pressing. The thickness of the nylon-6 interlayer was predetermined by placing

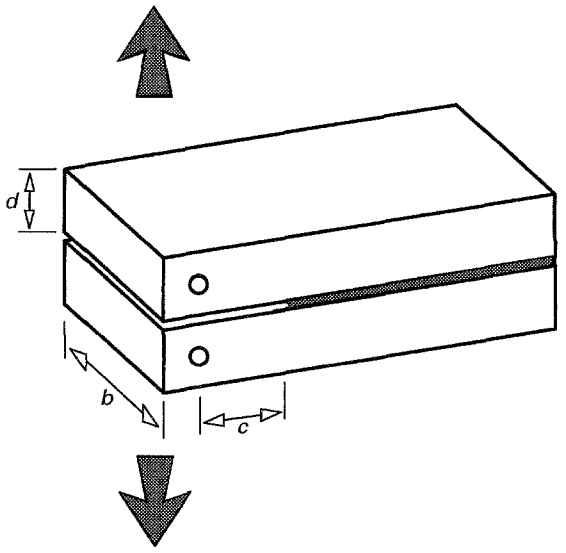

Figure 3 A double cantilever beam (DCB) geometry. The breadth and thickness of the specimen are $b = 25$ mm and $d = 10$ mm, respectively.

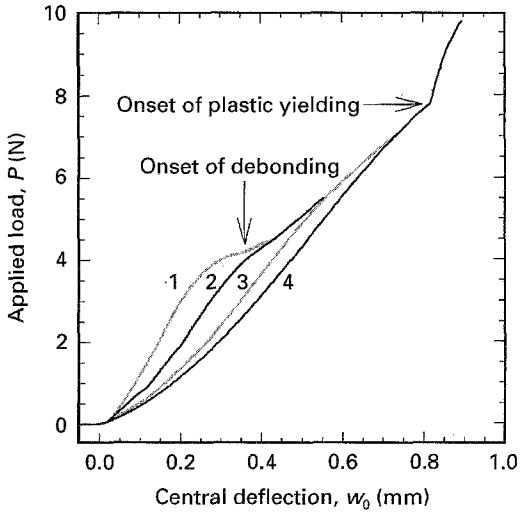

Figure 4 External load P as a function of blister central deflection w_0 (vertical shaft displacement). Curves 1–4 are four consecutive loadings of the same specimen. The onset of debonding of the first run is marked on the plot. The area covered bounded by any two curves represents the surface energy dissipated for the growing debonding area. Plastic deformation occurs when the stretching stress on the membrane reaches the yielding strength of nylon-6.

two aluminium strips of equal thickness at both ends of the aluminium bars. While a pressing load of 100–150 N was applied to the specimen, the temperature was raised to 230–240 °C and kept constant for 15 min. The specimens were ready when the melt cooled to room temperature. External load was applied via two drilled holes 7 mm from the free end of each cantilever arm and was measured as a function of central displacement, i.e. crack opening displacement, using an Instron machine. The crack length was measured in the course of loading.

The effect on the adhesion energy upon variations of (a) nylon-6 interlayer thickness, (b) hold time at elevated temperature and hot-press temperature, and (c) water exposure time were investigated. To vary the nylon-6 interlayer thickness, space bars of thickness ranging from 0.2 to 1 mm were to separate the two sandwiching aluminium bars. When the nylon-6 melt solidified, the interlayer assumed the thickness of the space bar. To test the hot-press hold time, the temperature was held at 230 °C for the designated time interval before testing. To investigate the hot-press temperature, the specimens were held for 15 min at the designated temperature ranging from 220 to 350 °C. Heating above 350 °C led to substantial oxidation degradation of nylon-6. The specimens were then cooled in laboratory air to room temperature. To test the durability of the nylon-6/aluminium interface in water, a number of specimens were prepared at 240 °C for 15 min. The samples were then fully immersed in cold tap water and individually removed from the bath and tested at their respective time intervals of 2, 4, 8, 11 and 14 days.

3. Results and analysis

3.1. Shaft-loaded blister

A plot of P versus w_0 for a typical specimen is shown in Fig. 4. The loading and unloading cycle were repeated four times. As the shaft was pushed into the blister at a small load, the blister "inflated" with its axisymmetric boundary remaining at the circumference of the bored vent. As the applied load was raised to a certain threshold P^*, debonding took place and the slope of the P–w_0 response decreased significantly. An almost linear P–w_0 response followed. The pre-debonding stage and the debonding stage were clearly identified in every loading curve. When the external load was removed, the blister returned to its original shape and w_0 dropped to zero. The blister was reloaded, but followed a different path to the critical debonding transition where the debonding front had stopped previously. Debonding followed. Four such consecutive loading curves (1–4) for a typical specimen were shown in Fig. 4. When the applied load was increased beyond a certain threshold (curve 4), the P–w_0 response distinctly turned due to plastic yielding. Such a critical transition from elastic-to-plastic response was observed in almost every specimen. Debonding continued as the applied load increased further. However, the rate of crack growth diminished, as a certain saturation limit of the debonding front was approached. The last stage of the blister loading resulted in piercing the blister at the centre, as predicted for a thin perfectly plastic polymer film [11]. Fig. 5a to c show the experimental data $w_0(P)$, $a(w_0)$ and $a(P)$, respectively, of a typical specimen with no surface treatment of the aluminium substrate.

The specific energy of adhesion W for a shaft-loaded blister test of a thin flexible membrane adhered to a rigid substrate has been obtained in our previous work [11] and is outlined in Appendix A. For a blister debonding undergoing elastic stretching (but without bending) deformation, we obtain

$$W \approx \frac{1}{\pi^2 Eh}\left(\frac{P}{w_0}\right)^2 \qquad (1a)$$

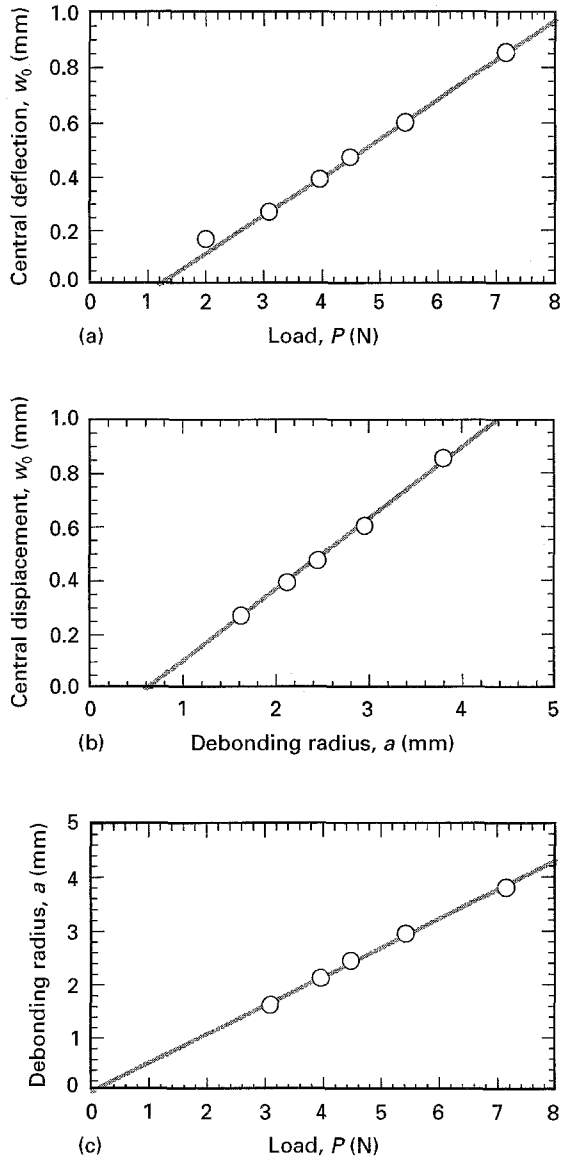

Figure 5 The measured blister central deflection w_0, debonding radius a and external load P of one typical specimen with no surface treatment on the aluminium substrate: (a) w_0 as a function of P; (b) w_0 as a function of a; (c) a as a function of P. In all three cases, a linear relationship is obtained.

$$\approx \frac{Eh}{16}\left(\frac{w_0}{a}\right)^4 \tag{1b}$$

$$\approx \left(\frac{1}{16\pi^4 Eh}\right)^{1/3}\left(\frac{P}{a}\right)^{4/3} \tag{1c}$$

where E and h are the elastic modulus and thickness of the membrane, respectively. The functions $w_0(P)$, $a(w_0)$ and $a(P)$ are thus predicted to follow a linear relationship. The linear relationships are verified in Fig. 5a to c. Once Equation 1 is satisfied, debonding occurs. For some tough interfaces, the membrane was pierced by the shaft before any debonding took place.

There is an alternative way to measure W. For an elastic blister of initial radius a_i, increasing external load traces a path $P_i(w_0)$ during the first loading (Fig. 4). Free inflation of the blister continues until the applied load reaches a threshold $(P^*)_{a_i}$ when debonding begins. The maximum elastic energy stored in the blister with a radius a_i is given by

$$(U_E)_{a_i} = \int_{P=0}^{P=P^*} P_i(w_0)\,\mathrm{d}w_0\Big|_{r=a_i} \tag{2}$$

Further increase in P leads to debonding and further inflation of the blister. If the final load and debonding radius are $(P^*)_{a_i}$ and a_f, respectively, the area under this section from $P = (P^*)_{a_i}$ to $P = (P^*)_{a_f}$ is therefore the sum of the debonding energy and the elastic energy of a larger blister of various radii. Now the external load is removed and reloaded from $P = 0$ to $P = (P^*)_{a_f}$ and a loading of $P_f(w_0)$ is traced. The area under this curve is the elastic energy stored in the blister of radius a_f. The amount of surface energy expenditure in expanding the blister from a_i to a_f is therefore given by the area A_{if} bounded by $P_i(w_0)$ and $P_f(w_0)$, and the specific debonding energy becomes $W = A_{if}/\pi(a_f^2 - a_i^2)$. This technique is generally known as the work area method applicable to elastic fracture of solids and best exemplified by the book by Atkins and Mai [16]. Either the indentation Equation 1 or the work area method yields similar W. Hereafter we will present only the indentation results using Equation 1.

The debonding energies of nylon-6 film from the aluminium substrate are summarized in Fig. 6. The three sets of results in each surface treatment correspond to (a) measurements made in laboratory air a few hours after the deposition, (b) debonding assisted by liquid water, (c) ageing for 10 months. The data scatter is over a large range. However, the "relative" W measured under dry and wet conditions and after ageing are fairly consistent from one specimen

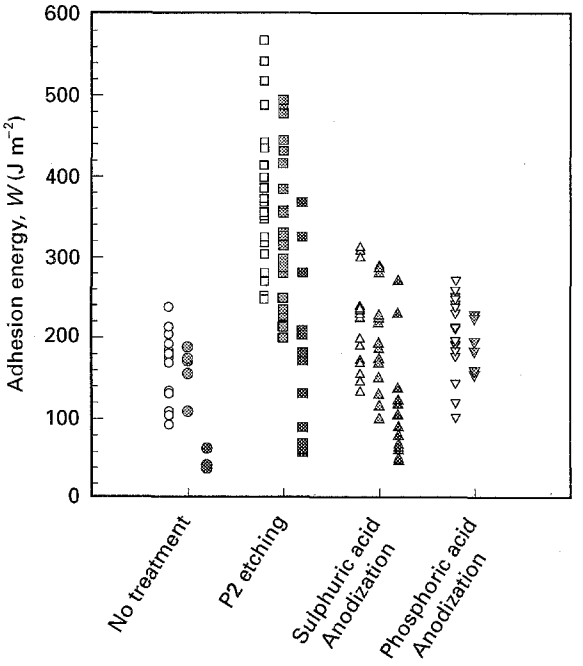

Figure 6 Debonding energy of nylon-6/aluminium interface for several surface treatments of aluminium surfaces. Open symbols denote debonding energy measured shortly after the specimens are prepared; shaded symbols show measurements in liquid water; dark symbols show measurement in laboratory atmosphere 10 months after specimen preparation.

to another. The P2 etched specimens show the best adhesion under all three conditions, followed by sulphuric acid anodization and phosphoric acid anodization. The plain aluminium surfaces show the weakest adhesion with nylon-6.

For a plain aluminium specimen, W varies in the range from 90 to 240 J m^{-2}. In the presence of water, some individual specimens show a weakened adhesion of 4–5% smaller than in the dry condition, while others no longer sustain an axisymmetric blister geometry. The debonding front grows in an unpredictable geometry in some cases. After a period of 10 months, adhesion of nylon-6 in these specimens almost fades away completely, dropping significantly to a low of 30 to 60 J m^{-2}, barely 10 per cent of the original strength in some cases.

In P2 etched specimens, adhesion is strongest among all surface treatments in this study. W varies in the range from 200 to 560 J m^{-2} and perhaps even higher in some individual specimens where debonding was not observed. Severe plastic deformation occurred prior to debonding. In the strongest adhered specimens, the blister crack never grew out of the initial radius, but piercing of the membrane was observed. This sets a lower bound to W of 600 J m^{-2}. The debonding front was somewhat difficult to locate in the P2 etched specimens because of the tarnished aluminium surfaces. In the presence of water, all specimens show a drop of approximately 80 J m^{-2}, i.e. the new W is about 80% of the original adhesion strength. A period of 10 months elapsed, the adhesion of nylon-6 on aluminium surfaces deteriorated by 30 to 75%. There was no significant difference between specimens with 2, 4, 5, and 6 min of surface treatments, except that the 1 min treatment gave a slightly smaller adhesion. Raman spectrum of the aluminium substrate after debonding showed the presence of nylon-6, but not on specimens with other surface treatments. At the melting temperature, nylon-6 fingers "anchored" well onto the pits on the substrate.

With anodized aluminium surfaces in sulphuric acid, W varies in the range from 130 to 300 J m^{-2}. In the presence of water, all specimens show a drop of 20–40 J m^{-2} from the original adhesion strength. The consequence of ageing leads to a spectrum of responses. Some specimens retained the original adhesion strength as if no deterioration was present. W in some dropped significantly to a level similar to that of the untreated plain aluminium surfaces. The rest dropped by a small amount of about 10–20 J m^{-2}.

With anodized aluminium surfaces in phosphoric acid, adhesion of nylon-6 is only slightly better than plain surfaces. W varies in the range from 100 to 270 J m^{-2}. In the presence of water, most specimens show a drop of 30–40 J m^{-2} from the original adhesion strength.

3.2. DCB configuration

The crack growth in the DCB configuration was in an intermittent fashion. In this section we calculate the adhesion energy using the maximum load at crack initiation, i.e. fracture toughness G_{1C} [17]:

$$W = G_{1C} = \frac{4F^2(3c^2 + d^2)}{E_{Al}b^2d^3} \quad (3)$$

where c is the crack length in the specimen; b and d are the dimensions of the aluminium bars as shown in Fig. 3; E_{Al} is the elastic modulus of aluminium which is taken to be 69 GPa.

Since the adhesion is shown in the previous section to be the strongest with the P2 etched aluminium surface, DCB experiments were conducted only on such interfaces. Adhesion energy varies from 200 to 500 J m^{-2} over the specimen samples even though the aluminium surface treatment is identical, which is consistent with the measurements obtained by the blister test. Because of the large data scatter, we will only show an individual set of data in this section.

3.2.1. Thickness of nylon-6 interlayer

In specimen preparation, the pre-crack was made to be within the nylon-6 interlayer. However, there are two distinguished modes of fracture in the DCB tests: (a) cohesive interface failure, where the crack continued to propagate through the nylon-6; and (b) adhesive interface debonding, where the crack ran into the nylon-6/aluminium dissimilar interface soon after it began to propagate. Such phenomena were shown remarkably in the film thickness variation experiments.

Fig. 7a shows the fracture energy measured as an increasing function of nylon-6 film thickness. When the film is thin, cohesive interface failure dominates. As the thickness increases beyond a threshold, adhesive failure prevails. The experiments were repeated several times with the same aluminium surface treatment and other treatments, and the same cohesive/adhesive failure transition occurs at the same threshold. Though adhesive layer thickness does not usually affect adhesion, it has a significant effect when the plastic zone around the debonding front is large. With relatively thin adhesive layers the presence of high modulus and high yield strength substrates, such as aluminium alloys, may restrict the full volume of the plastic zone from developing in the adhesive layer. Thus cohesive failure in the nylon-6 adhesive is expected and so is a decreasing adhesion energy when the adhesive layer is smaller than a certain threshold. As shown in Fig. 7a, the critical thickness is approximately 0.6 mm. The specimens prepared for the subsequent experiments were made to have the nylon-6 layer thicker than this critical value in order to enhance crack propagation at the nylon-6/aluminium interface.

3.2.2. Hold time and hot-press temperature

The fracture toughness of the interface is significantly controlled by the hot-pressing time and temperature. The dependence is shown in Fig. 7b and c, respectively. The fracture strength of the nylon-6/aluminium interface increases as either quantity increases, followed by a sudden drop after passing a critical threshold hold

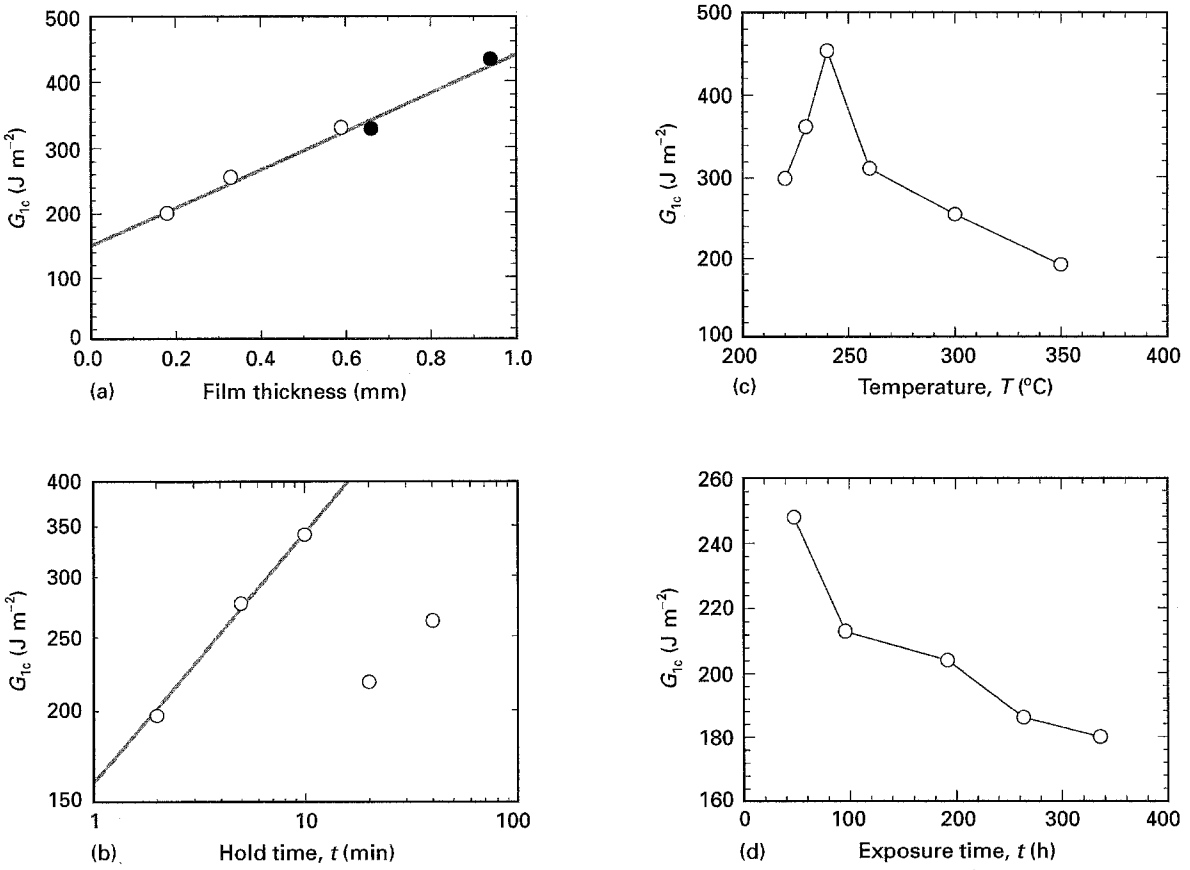

Figure 7(a) Fracture toughness of nylon-6/aluminium interface as a function of nylon-6 interlayer thickness. The crack runs into nylon-6 interlayer (open symbols) when the interlayer is thin, while debonding occurs at the dissimilar interface (dark symbols) for thick nylon-6 films. (b) Fracture toughness of nylon-6/aluminium interface as a function of holding time at hot-press temperature. The linear portion of the log–log plot gives an approximate slope of 0.3. Subsequent drop of fracture toughness is due to oxidation degradation of the nylon-6 interlayer. (c) Fracture toughness of nylon-6/aluminium interface as a function of hot-press temperature. A linear increase in fracture toughness at low temperature is followed by a sudden decrease due to oxidation degradation of the nylon-6 interlayer. (d) Fracture toughness of nylon-6/aluminium interface as a function of water exposure time.

time or temperature. It was noted that the nylon-6 was oxidized when it was held at the melting temperature for a long enough time. Thermal degradation/oxidation reduces the fracture toughness.

When a polymer is melted, its viscosity lowers and the wettability increases [3]. The reduction of contact angle allows the polymer melt to flow into the surface pits of the aluminium surface which enhances capillary penetration of the melt and creates mechanical interlocking anchors. Newman [18] proposed a model with the time dependent contact angle as a function of the surface tension of the polymer liquid to its vapour, the flow viscosity, and range of interfacial interaction. Based on this theory, Wu [19] argued that the rate of adhesive strength S (or W) development in many systems obeys a simple relation

$$S = At^b \quad (4)$$

where A and b are some constants with the latter in the range between 1/4 and 1/5. Viscosity and dynamic contact angle of nylon-6 at elevated temperature are well documented. In Fig. 7b, the best fit value for b is 0.3 which agrees reasonably well with the theory.

The hot-press temperature dependence of the fracture strength is believed to be the consequence of lowered viscosity at elevated temperature. Provided there is no degradation of the nylon-6 interlayer due to oxidation at high temperature, the capillary penetration of the polymer into the surface pits yields better macroscopic adhesion.

3.2.3. Durability

The mechanical properties of nylon-6 is notorious for its dependence on its water content [12]. The interface strength deteriorates as the time of exposure to water is lengthened (Fig. 7d). Environmental assisted crack growth is well documented in many engineering materials [16, 20–24]. The weakening of adhesion at the interface in the presence of water is believed to be the consequence of dielectric shielding of electrostatic attraction, cleavage of strong covalent bonds, chemical reaction, etc. In polymer/metal interfaces, the hydrogen bonding between metal oxide and polymer chain molecules is much weakened in a dielectric medium such as water. In our blister specimens, diminished adhesion was observed in moist air. Capillary condensation of water molecules [25] in the surface pits and debonding front is thought to play an important role.

4. Conclusions

Of the three aluminium surface treatments: P2 etching process, sulphuric acid anodization and phosphoric acid anodization, P2 is the most effective in bonding

nylon-6 onto aluminium substrate. 3-D mechanical interlocking between the polymer and metal is the main reason for effective adhesion.

Appendix A: Derivation of the specific work of interface adhesion *W*

Here we present a brief outline of the derivation of W while the detailed version will be published elsewhere [11]. For a thin flexible blister elastically stretched by a central point load (Fig. 2a), the work of the applied load is given by

$$U_P = -Pw_0 = -2\pi \int_0^a q(r)w(r)r\,dr \qquad \text{(A1)}$$

where $w(r)$ represents the blister geometry, assumed to be conical

$$w(r) = w_0\left(1 - \frac{r}{a}\right) \qquad \text{(A2)}$$

and $q(r)$ is defined to be

$$q(r) = \frac{1}{r}\frac{d}{dr}(r\Psi) \qquad \text{(A3)}$$

with the load function $\Psi = P/2\pi r$ for a central point load. The elastic energy of stretching stored in the elastic medium is given by

$$U_E = 2\pi \int_0^a (N_r\varepsilon_r + N_t\varepsilon_t)r\,dr \qquad \text{(A4)}$$

where N and ε are the membrane stress and strain, respectively, and the subscripts r and t denote the radial and tangential components. By the principle of virtual work, $\delta U_E + \delta U_P = 0$, we obtain

$$4Pa^2 \approx \pi E h w_0^3 \qquad \text{(A5)}$$

For a debonding blister in equilibrium, the energy required to expose an area πa^2 is $U_S = \pi a^2 W$. Energy balance requires $\delta U_E + \delta U_P + \delta U_S = 0$ with respect to the debonding area πa^2, which implies (using Equation A5)

$$W \approx \frac{1}{\pi^2 Eh}\left(\frac{P}{w_0}\right)^2 \qquad \text{(A6)}$$

which is Equation 1a.

Acknowledgements

This research was funded by the Australian Research Council. The authors are grateful to Dr M. V. Swain and Mr T. Bell at the National Measurement Laboratories of CSIRO in Sydney, Australia for access to the indentation facilities, and Mr C. H. Lee at the Department of Mechanical Engineering in Hong Kong University of Science and Technology for technical advice.

References

1. P. S. HO, R. HAIGHT, R. C. WHITE, B. D. SILVERMAN and F. FAUPEL, in "Fundamentals of Adhesion", edited by L.-H. Lee (Plenum, New York, 1991) p. 383.
2. A. M. STONEHAM, M. M. D. RAMOS, and A. P. SUTTON, *Phil. Mag. A.* **67** (1993) 797.
3. D. E. PACKHAM, in "Adhesion Aspects of Polymeric Coatings", edited by K. L. Mittal (Plenum, New York, 1983) p. 19.
4. J. P. BELL, R. G. SCHMIDT, A. MALOFSKY and D. MANCINI, *J. Adhesion Sci. Technol.* **5** (1991) 927.
5. J. SCHULTZ, *J. Adhesion* **37** (1992) 73.
6. J. E. E. BAGLIN, in "Fundamentals of Adhesion", edited by L.-H. Lee (Plenum, New York, 1991) p. 363.
7. K. KENDALL, *J. Phys. D: Appl. Phys.* **8** (1975) 1449.
8. L. G. ROSENFELD, J. E. RITTER, T. J. LARDNER and M. R. LIN, *J. Appl. Phys.* **67** (1990) 3291.
9. H. DANNENBERG, *J. Appl. Polym. Sci.* **5** (1961) 125.
10. M. L. WILLIAMS, *ibid.* **13** (1969) 29.
11. K-T. WAN and Y.-W. MAI, *Int. J. Fract.*, in press.
12. W. E. NELSON, "Nylon Plastics Technology" (Newnes-Butterworths, London, 1976).
13. M. I. KOHAN, "Nylon Plastics" (John Wiley & Sons, New York, 1973).
14. J. C. BOLGER, in "Adhesion Aspects of Polymeric Coatings", edited by K. L. Mittal (Plenum, New York, 1983) p. 3.
15. R. F. WEGMAN, "Surface Preparation Techniques for Adhesive Bonding" (Noyes, New Jersey, 1989) Ch. 2.
16. A. G. ATKINS and Y.-W. MAI, "Elastic and Plastic Fracture" (Ellis Horwood/John Wiley, Chichester, UK, 1985).
17. H. TADA, P. C. PARIS and G. R. IRWIN, "The Stress Analysis of Cracks Handbook" (Del Research Corporation, St. Louis, 1985).
18. S. NEWMAN, *J. Colloid Interf. Sci.* **26** (1968) 209.
19. S. WU, "Polymer Interface and Adhesion" (Marcel Dekker, New York, 1982).
20. J. S. AHEARN, G. D. DAVIS, T. S. SUN, and J. D. VENABLES, in "Adhesion Aspects of Polymeric Coatings", edited by K. L. Mittal (Plenum, New York, 1983) p. 281.
21. HATSUO ISHIDA, in "Adhesion Aspects of Polymeric Coatings", edited by K. L. Mittal (Plenum, New York, 1983) pp. 45–105.
22. D.-C. HU and H.-S. CHEN, *J. Adhesion Sci. Technol.* **6** (1992) 527.
23. K. K. KNOCK and M. C. LOCKE, in "Adhesion Aspects of Polymeric Coatings", edited by K. L. Mittal (Plenum, New York, 1983) p. 301.
24. Y.-W. MAI, *J. Adhesion* **7** (1975) 141.
25. K.-T. WAN and B. R. LAWN, *Acta. Metall. Mater.* **38** (1990) 2073.

Received 12 January
and accepted 4 October 1995